



# Evaluation of simulated N cycling using observations from a $^{15}\text{N}$ tracer experiment in a mixed deciduous forest

Tea Thum<sup>1</sup>, Christine L. Goodale<sup>2</sup>, Lin Yu<sup>3</sup>, Julia Nabel<sup>4</sup>, and Sönke Zaehle<sup>4</sup>

<sup>1</sup>Department of Climate System Research, The Finnish Meteorological Institute, Helsinki, Finland

<sup>2</sup>Department of Ecology and Evolutionary Biology, Cornell University, Ithaca, NY, USA

<sup>3</sup>Department of Earth System Sciences, University of Hamburg, Hamburg, Germany

<sup>4</sup>Biogeochemical Signals Department, Max Planck Institute for Biogeochemistry, Jena, Germany

**Correspondence:** Tea Thum (tea.thum@fmi.fi)

**Abstract.** Nitrogen availability constrains the terrestrial carbon uptake and storage, yet large uncertainties remain in the magnitude of the effect, because the interactions of the carbon and nitrogen (N) dynamics are challenging to observe in undisturbed ecosystems at relevant timescales. Long-term experiments with  $^{15}\text{N}$  tracer applications allow study of the nitrogen cycle in a fairly undisturbed manner, and they are therefore a valuable data source to test the biogeochemical dynamics simulated by terrestrial biosphere models. In this study we applied the model QUINCY (QUantifying Interactions between Terrestrial Nutrient CYcles and the climate system), which includes an explicit representation of terrestrial  $^{15}\text{N}$  fluxes and pools. We used observations from a long-term (10-year)  $^{15}\text{N}$  tracer experiment in a temperate deciduous forest to evaluate the nitrogen dynamics simulated by QUINCY. Recovery in soil N dominated overall ecosystem  $^{15}\text{N}$  recovery in both observations and simulations over the long-term. The observed gradual movement of the  $^{15}\text{N}$  tracer to lower soil layers was also captured by the model. However, in the short-term modeled uptake and losses of  $^{15}\text{N}$  into leaves and fine roots were too fast, and recovery in litter and surface soil was too slow, indicating that the model likely overestimates plant competitiveness for newly added N relative to soil microbes. Downward vertical transport of  $^{15}\text{N}$  tracer in the soil was slow compared to measurements, which may be indicative either of too low bioturbation or vertical transport via leaching. Overall, the QUINCY model results showed good agreement with the observations making it a valuable tool to study long term nitrogen dynamics. Running the model for an extended period for example indicated that the ecosystem retained a very large share of the added  $^{15}\text{N}$  tracer (>90 %), and that this retention persisted at multi-decadal timescales. This study shows that explicit inclusion of isotopic tracers allows for a more profound evaluation of carbon-nitrogen turnover and dynamics and thereby can contribute to reduce uncertainties in modelling nitrogen flow and constrains in terrestrial ecosystems.



## 20 1 Introduction

Climate change influences plant-atmosphere interactions as ecosystems face new conditions due to increasing atmospheric CO<sub>2</sub> and changing climate (Canadell et al., 2022). It is crucial to have a better understanding of the capacity of vegetation to take up atmospheric CO<sub>2</sub> and the fate of terrestrial carbon (C) storage, as potential feedbacks may attenuate or further accelerate climate change. The bio-availability of nitrogen (N) has a pivotal role in the carbon sink potential of vegetation and  
 25 soils, as N is scarce in many ecosystems given limited inputs from atmospheric deposition and biological nitrogen fixation (LeBauer and Treseder, 2008), but plants require N in the photosynthetic machinery and to construct new biomass (Bonan, 2016). Understanding the role of the N cycle on the terrestrial C cycle is especially important as terrestrial N limitation is expected to intensify in response to the increasing atmospheric CO<sub>2</sub> (Rogers et al., 2017).

At the same time, humans have not only perturbed the C cycle, but also the natural N cycle by industrial combustion  
 30 processes as well as agricultural fertilization (Gruber and Galloway, 2008). The amount of reactive N has increased and led to increased N deposition across many parts of the world (Galloway et al., 2008). These anthropogenic influences on the nitrogen cycle have diverse effects on natural ecosystems, such as eutrophication, air pollution and biodiversity loss (Gong et al., 2024; Schlesinger, 2009). Increased N deposition also influences C sequestration, such as stimulation of tree growth and altered soil decomposition processes (Zaehle and Dalmonech, 2011). The magnitude of the effect of N deposition in forests has been  
 35 debated (Gurmesa et al., 2022; Magnani et al., 2007; Sutton et al., 2008; Reay et al., 2008). The global N-induced increases in forest net carbon uptake have been estimated to be in the range of 130–345 TgCyr<sup>-1</sup> by several studies using different approaches (de Vries et al., 2014; Du and de Vries, 2018; Fleischer et al., 2019; Jain et al., 2009; Quinn Thomas et al., 2010; Schulte-Uebbing and de Vries, 2018; Wang et al., 2017; Zaehle and Dalmonech, 2011), with smaller recent estimate of 41 TgCyr<sup>-1</sup> from a data-based approach (Schulte-Uebbing et al., 2022). An important uncertainty in the response of the carbon  
 40 cycle to additions of N is the fate of the extra N in the ecosystem (Nadelhoffer et al., 1999b). The response depends on the fraction of N that is retained in the ecosystem rather than lost to leaching or gaseous losses, and the partitioning of the retained nitrogen into pools with a narrow C:N ratio, such as soil organic matter, or a wider C:N ratio, such as woody biomass (Gurmesa et al., 2022; Nadelhoffer et al., 1999b). Knowing the fate of the incoming N to the ecosystem is therefore crucial.

Terrestrial biosphere models (TBMs) are useful tools in predicting the trajectories of terrestrial C stocks in soil and vegetation  
 45 (Friedlingstein et al., 2025; Seiler et al., 2022), as they in principle can account for the numerous interactions between the N and C cycles. However, modelling of the N cycle is challenging, as many processes are involved but comprehensive data sets to evaluate the models are scarce (Meyerholt et al., 2020), since measuring many aspects of the N cycle is difficult (Vicca et al., 2018). Results from manipulation experiments, including both N fertilization and tracer addition studies, are important resources for the further evaluation and development of the N cycle description in the TBMs (Thomas et al., 2015).

50 N fertilization experiments in forests have a long history, the earliest originating from the early 20th century (Högberg et al., 2017). These experiments have been valuable in estimating optimal N fertilization for forest management as well as in increasing the understanding of the N cycle in these ecosystems. These data have also been used in model development (Meyerholt and Zaehle, 2015; Caldararu et al., 2020). However, these experiments have limitations, as fertilized ecosystems



are no longer in their natural state, and fertilization may lead to N saturation or species replacement (LeBauer and Treseder, 2008; Van Houtven et al., 2019). In model development it is often preferable to have observations of the ecosystems at their natural state. Additionally, it is difficult to trace the effect of individual N cycle processes beyond the effect on tree biomass, although such insights are needed to further increase our understanding and improve model representation.

Isotopic tracer experiments can overcome these issues, as very small additions of nitrogen as highly enriched  $^{15}\text{N}$  are enough to allow the tracer to be tracked across different soil and vegetation pools (Buchmann et al., 1995; Lin et al., 2024; Nadelhoffer et al., 1999a; Schleppi and Wessel, 2021). Traditionally these observations are challenging and expensive to make, however, improved measurement techniques have made these observations more frequent, offering more data (Schleppi and Wessel, 2021) that can also be used for model development. These observations have revealed many important aspects of the nitrogen cycle that would otherwise have been challenging to address (Craine et al., 2015; Robinson, 2001), for example the uptake of N by the forest canopy has been quantified (Ferraretto et al., 2022; Da Ros et al., 2023; Li et al., 2025).

These isotopic tracer experiments have been used in testing models without an explicit  $^{15}\text{N}$  cycle (Cheng et al., 2019; Thomas et al., 2013) and have given insight to nitrogen turnover rates and competition for N between plants and soil microbes. A more direct use of these  $^{15}\text{N}$  observations is to compare them with the  $^{15}\text{N}$  cycle if explicitly described in a model, as it is done in the TBM QUINCY (QUantifying Interactions between terrestrial Nutrient CYcles and the climate system) (Thum et al., 2019). QUINCY has already been used in Caldararu et al. (2022) to explain the drivers of long-term trends in natural abundance measurements of  $^{15}\text{N}$  in plant tissues. In the present study, we compare QUINCY to a  $^{15}\text{N}$  tracer experiment in a temperate mixed deciduous forest, where the fate of the applied  $^{15}\text{N}$  tracer has been studied for a decade after the experiment. We specifically want to evaluate the temporal dynamics of the signal in different pools during an 11-yr period, the partitioning of the  $^{15}\text{N}$  signal across different ecosystem compartments, how well the model reproduces these patterns, and what potential developmental needs this assessment offers for nitrogen cycle modelling. Also, we want to study in a simulation experiment what the fate of the  $^{15}\text{N}$  is at decadal time scales, to consider the impact of N input on the carbon pools of the ecosystem. In particular, we address the following research questions:

- How realistic are the simulated plant N pool turnover rates?
- How well can we simulate retention of the  $^{15}\text{N}$  tracer in the ecosystem?
- How long will the  $^{15}\text{N}$  tracer stay in the ecosystem and where will it end up?

## 2 Materials and methods

### 2.1 $^{15}\text{N}$ experiment and the experiment site

#### 2.1.1 Site description

The Arnot Forest (42 ° 17' N, 76 ° 38 W', 503 m elevation) is located in central New York State, the U.S. The annual mean temperature is 7.8 °C and the annual mean precipitation 930 mm (Goodale, 2017). Total atmospheric N deposition averaged



85 8-10 kg N ha<sup>-1</sup> yr<sup>-1</sup> during 2000-2013 (Butler et al., 2015). The forest consists mostly of second-growth mixed hardwoods established naturally after harvest in 1873-1887 and fires in 1900-1911 (Fain et al., 1994). The dominant species include white ash (*Fraxinus americana*), red maple (*Acer rubrum*), quaking aspen (*Populus tremuloides*), basswood (*Tilia americana*) and some eastern hemlock (*Tsuga canadensis*) (Goodale, 2017). The soil structure consists of 18 % clay, 41 % silt and 40 % sand and the pH is 4.4, measured at the 0-10 cm depth (Fahey et al., 2013). Leaves usually emerge in early to mid May and most  
 90 leaf fall by the end of October.

### 2.1.2 Tracer addition experiment

In 2007, 0.21 kg ha<sup>-1</sup> of <sup>15</sup>N tracer was applied as 99 atom % <sup>15</sup>N–KNO<sub>3</sub>, split into equal applications of 0.07 kg ha<sup>-1</sup> applied on 30 April, 31 July and 30 October (Goodale et al., 2015). The total amount of the three applications equals <3% of one year of nitrogen deposition at the site. The tracer was sprayed on the forest floor. Measurements of <sup>15</sup>N in fine and coarse  
 95 roots located in the upmost soil layer (0-10 cm depth) were conducted in late November 2007. Tree N and <sup>15</sup>N pools (foliage, wood, bark, coarse and fine roots) and soil pools down to 50 cm were measured one year before and after the tracer additions, in summers 2006 and 2008. Later measurement occurred in 2012-2013 (5-6 years after tracer addition), when soil and root samples were taken in October 2012 and the aboveground pools were sampled in June 2013. The last measurements of the plant and soil <sup>15</sup>N pools were collected in 2017, 10 years after the tracer addition. The wood pools were not measured at this  
 100 point.

The fraction (as %) of added <sup>15</sup>N tracer in each of the pools <sup>15</sup>N<sub>Rec</sub> was computed using each pool's N storage (M<sub>poolN</sub>) and the change in mean atom <sup>15</sup>N after the tracer addition (<sup>15</sup>N<sub>post</sub>) relative to the mean pre-addition (<sup>15</sup>N<sub>pre</sub>) and the total mass of added tracer (M<sub>15Nadded</sub>):

$$^{15}\text{N}_{\text{Rec}}(\%) = \frac{(\text{atom}\%^{15}\text{N}_{\text{post}} - \text{atom}\%^{15}\text{N}_{\text{pre}}) * M_{\text{poolN}}}{M_{^{15}\text{Nadded}}} * 100 \quad (1)$$

### 105 2.2 Model description of QUINCY

QUINCY is a terrestrial biosphere model that simulates the energy, water, carbon and nutrient (nitrogen and phosphorus) cycles (Thum et al., 2019). For simplicity, in this study we apply the model with soil phosphorus availability set to non-limiting levels, such that plant and soil biogeochemical processes operate at average observed P contents. Parallel to the nitrogen cycle, a representation of the <sup>15</sup>N cycle has been implemented, largely following the description of discrimination processes by  
 110 Robinson (2001). Different ecosystems are represented using different plant functional types (PFTs).

We outline here some of the basic characteristics of the model, and a full description of the model can be found in Thum et al. (2019). Plants contain three fast-lived pools (leaves, fine roots and fruits), a non-structural pool (reserve) and a seasonal, non-respiring pool (labile), along with three structural tissue types (sapwood, heartwood and coarse roots). All vegetation and soil pools in the QUINCY model contain carbon, nitrogen and <sup>15</sup>N. Photosynthesis in the multi-layered canopy is calculated  
 115 following the formulation by Kull and Kruijt (1998). Photosynthetic parameters depend on the leaf N concentration (Friend



et al., 1997). Leaf mass and N concentrations respond to soil N availability (Hyvönen et al., 2008). Plant nutrient uptake depends on fine root biomass, soil mineral nutrient concentration and plant nutrient demand.

The newly acquired carbon, nitrogen and  $^{15}\text{N}$  are first placed in the labile pool, from which they can be used for new growth of tissues, respiration or storage in the reserve pool. The potential growth rate is influenced by the PFT-specific allometric relationships between leaves, sapwood and fine and coarse roots. Belowground carbon allocation increases under nutrient or water stress. Actual growth is further controlled by the nutrient demand of each plant pool, the nutrients available for growth and it can be limited by air temperature and soil moisture. Flexible stoichiometry is allowed for leaves and fine roots.

The simulated soil has a vertically layered structure, with 15 layers of exponentially increasing soil depth down to 9.5 m. The soil biogeochemical processes largely follow the CENTURY model approach (Parton et al., 1993). Each soil layer has organic pools, consisting of metabolic (soluble), structural (polymeric), and woody litter pools, fast and slow overturning organic matter (SOM), and inorganic ammonium ( $\text{NH}_4$ ) and nitrate ( $\text{NO}_3$ ) pools. The litter and SOM pool turnover rates are dependent on soil temperature and moisture, described by first-order kinetics functions. The stoichiometry of the litter pools is determined by the respective plant pool stoichiometries along with the plant resorption capacity for each nutrient. The fraction of resorption to the labile pool for leaves before shedding is 50 % and for wood 20 % during conversion of sapwood to dead heartwood. Fine root death is assumed to be dominated by predation and therefore no resorption occurs from them. The fast SOM pool stoichiometry for C:N is affected by available inorganic N while the slow SOM pool stoichiometry is assumed to be fixed. Plants and microbes compete over the inorganic nutrients, determined by their nutrient demand. Nitrification and denitrification processes depend on the aerobic status, temperature and moisture in each soil layer (Zaehle and Dalmonech, 2011). Biological nitrogen fixation (BNF) calculation is based on plant demand and the relative costs of root uptake of mineral nutrients and biological fixation (Meyerholt et al., 2016). As a further development to the baseline version of the model (Thum et al., 2019), nitrate assimilation of soil microorganisms (i.e. immobilisation of nitrate from the solute pool to the fast soil pool) was implemented. While this allows more rapid uptake of  $^{15}\text{N}$  from nitrate in the soil, this change has overall limited impact on the model results, as N immobilisation by microbial growth is primarily determined by the stoichiometric imbalance between litter and SOM as well as the potential litter decomposition rate in the model.

Isotopic discrimination of  $^{15}\text{N}$  occurs during biological nitrogen fixation, ammonification, plant and microbial N uptake, and processes associated with nitrification and denitrification. Fractionation parameters were taken from Robinson (2001) (Table A1). Biomass growth and retranslocation of N are assumed to not fractionate N.

## 2.3 Model set-up

In this study the model was run at a site scale and the site was described with a summergreen broadleaf deciduous forest PFT. QUINCY runs at half-hourly timestep and requires as forcing variables air temperature, humidity, precipitation, air pressure, short- and longwave radiation, wind velocity, atmospheric  $\text{CO}_2$ ,  $^{13}\text{CO}_2$ ,  $^{14}\text{CO}_2$  mole fractions and  $\text{NH}_x$ ,  $\text{NO}_y$  and  $\text{PO}_4$  deposition rates. Further information needed for sites are geographical coordinates and soil physical and chemical parameters (texture, bulk density, rooting and soil depth, inorganic P content). The turnover rates of vegetation and soil pools for this PFT can be found in Table S1.



150 We made a model simulation for the Arnot forest using meteorological data from the CRU JRA v2.1 dataset (University of East Anglia Climatic Research Unit, 2020), which was disaggregated to half-hourly data using a statistical weather generator (Zaehle and Friend, 2010). The annual atmospheric CO<sub>2</sub> concentration was taken from Le Quéré et al. (2018) and N deposition data from Lamarque et al. (2010, 2011). The soil texture and pH were taken from the observations (Fahey et al., 2013). We did not include woody litter in the analysis, since it is not largely taking part in the  $\delta^{15}\text{N}$  cycle at the studied timescale.

155 First, a 1000-year-long spinup was performed by cycling driving data between the years 1901 and 1930. After this a model simulation was done for the years 1901 to 2018, using transient climate, CO<sub>2</sub> concentration and N deposition for the site. In the simulations the  $^{15}\text{N}$  tracer is placed as NO<sub>3</sub> solute in the uppermost soil layer at the same days as the tracer application was performed in the tracer addition experiment. For the scenario run extending further 30 years from the final year 2018, the climatic forcing was prepared using the current day climate and the CO<sub>2</sub> from the RCP 8.5 (Riahi et al., 2011).

160 Some additional sensitivity tests were performed to assess to which extent the simulation results depend on the assumed fraction of N retention during leaf senescence as well as the turnover rate of soil organic matter pools. In these tests we varied the coefficient determining the amount of nutrients being taken back to the reserve pool before leaf senescence, or increased the turnover rates of the soil pools, that would cause them to be smaller. Because these changes affected the overall model performance without yielding improved correspondence to the observed characteristics of the carbon and nitrogen cycle, and

165 without strong effects on the temporal evolution of the tracer distribution we simply applied the model using the default parameters for this PFT instead of rigorous parameter tuning.

### 3 Results

#### 3.1 Comparison between magnitudes of observed and simulated pools and fluxes

First, we investigate the overall model performance in reproducing observed characteristics of the Arnot site - vegetation and

170 soil pools as well as C and N fluxes - because differences in pools between the observations and simulations will influence the  $\delta^{15}\text{N}$  values from the tracer experiment (Table 1): If a pool is overestimated in the simulations, the magnitude of the  $^{15}\text{N}$  signal will be low-biased given the observation-based flux partitioning. It is important to note that the model has not been calibrated to this particular site and default parameter values have been used.

The N deposition was similar in the observations and input for the simulations that had been taken from Lamarque et al.

175 (2010, 2011). The simulated annual gaseous N fluxes were of the same magnitude as the observations, in particular considering that the uncertainty range of the observations is large. Although key indicators of productivity are comparable to the observations (wood production and leaf C, which is related to leaf area index), the model showed notable deviations from the observed partitioning of carbon and nitrogen in vegetation. The model underestimated the amount of below-ground carbon, specifically fine root biomass, while generally exhibiting a tighter C:N stoichiometry in leaves, root, and woody biomass. Discrepancies in

180 leaf litter fall are possibly the result of a combination of under-reporting in the observations in combination with the omission of the coniferous hemlock species in the model. Comparison of leaf mass and leaf litter fall stoichiometry suggests that leaf N resorption during leaf senescence was less than the assumed 50% in the model. In the observations, the mortality exceeded the



**Table 1.** Observed (in bold) and simulated carbon and nitrogen pools and fluxes. The simulated values are 20 year averages. Soil value refers to the top 50 cm of soil organic matter.

Storage	C (gC m <sup>-2</sup> )	N (gN m <sup>-2</sup> )	C:N
Leaf	<b>140</b> 120	<b>4.0</b> 5.3	<b>35</b> 23
Fine roots	<b>270</b> 62	<b>5.3</b> 2.7	<b>51</b> 27
Coarse roots	<b>810</b> 580	<b>6.8</b> 3.7	<b>119</b> 155
Wood	<b>9920</b> 12 009	<b>23</b> 75	<b>431</b> 160
Litter	<b>260</b> 366	<b>7.3</b> 3.6	<b>36</b> 101
Soil	<b>7600</b> 14 709	<b>737.4</b> 1652	<b>12</b> 9
Flux	C (gC m <sup>-2</sup> yr <sup>-1</sup> )	N (gN m <sup>-2</sup> yr <sup>-1</sup> )	C:N
Leaf litterfall	<b>96</b> 147	<b>1.5</b> 3.1	<b>63</b> 47
Mortality	<b>250</b> 129	<b>0.5</b> 0.9	<b>500</b> 143
Wood production	<b>154</b> 182	<b>0.5</b> 1.2	<b>334</b> 152
N <sub>2</sub> O flux	-	<b>0.006</b> 0.01	-
N <sub>2</sub> flux	-	<b>0.04-0.8</b> 0.31	-
N deposition	-	<b>0.7-0.9</b> 0.87	-

wood production, which was not reproduced by the model, which estimated that wood production and mortality were roughly balanced. The N flux of mortality was larger than the observed, probably because the observation-based estimate of mortality only accounted for the mortality of woody biomass, whereas the mortality term in the model also accounted for leaf, root and fruit biomass.

The litter (also denoted as Oi) C pool was overestimated in the simulations compared to the observations. Given the discrepancy between observed litter C:N and litter fall C:N, it appears likely that processes during litter decomposition already affected observed litter C:N, whereas the litter pool reported by the model was fresh, undecomposed litter. The simulations strongly overestimated soil C, as it was almost twice the observed value (Table 1), where the fast overturning pool contributed to 17 % of the total SOM C pool and 18% of the total SOM N pool. The SOM C:N ratio of the combined simulated fast and slow soil pools was similar to the observations. The observed soil C:N ratios declined strongly with soil depth, whereas - as per model assumption - the simulated soil C:N ratios remained nearly constant throughout the different soil layers (Table S2).

In the observations (Table S3), natural abundance  $\delta^{15}\text{N}$  of leaves (-2.1 ‰) and coarse roots (-2.4 ‰) were most depleted and the wood (-1.2 ‰) was the most enriched vegetation pools. The simulated  $\delta^{15}\text{N}$  in leaves (-2.3 vs. -2.1 ‰) and wood (-1.2 vs. -1.1 ‰) were similar to the observations. The simulated  $\delta^{15}\text{N}$  in coarse roots (-1.4 ‰) was not as depleted as in the observations (-2.4 ‰). The natural abundance  $\delta^{15}\text{N}$  levels in the litter layer and soil were more enriched than in the simulations, the difference being largest in the deepest soil layers (Table S3).





### 3.2 $\delta^{15}\text{N}$ signal: Temporal evolution

200 In the experiment the tracer was sprayed on top of the litter layer. In the simulations, we added the incoming tracer to the N deposition, from where it directly entered the soil solution  $\text{NO}_3$  pool of the uppermost soil layer. This slight difference may cause some discrepancies in the comparison, as in the model, the  $\text{NO}_3$  solute of the first soil layer is directly accessible to the vegetation and soil microbes. Given the time-scale of this analysis, however, we assume that the potential delay of accessibility for plants and soil microbial biomass due to the time-scale of transfer of the tracer from the litter layer into the soil, should not  
 205 strongly affect our results.

Fig. 1 shows the temporal change of the  $\delta^{15}\text{N}$  from reference value (year 2006) in different plant pools. The simulated values are shown at a daily time step until 11 years after the tracer application (Fig. 1); the original natural abundance values are shown in Table S3. Similar to observations, simulations showed a rapid  $\delta^{15}\text{N}$  enrichment of both leaves and fine roots in the year after the tracer was applied, but the simulated declines of  $\delta^{15}\text{N}$  enrichment over the next decade were faster and larger  
 210 than observed for these pools (Fig. 1). Simulated leaf  $\delta^{15}\text{N}$  enrichment (Fig. 1a) showed some small increases already in 2007, but reached its highest level in 2008 (hitherto, all values reported are relative to the initial natural abundance  $\delta^{15}\text{N}$ ), 51.4 ‰, the year after the tracer addition. One year later, the simulated  $\delta^{15}\text{N}$  enrichment decreased by more than 50 % and reached a steady low-level enrichment (5.9 ‰) by 2012. The observations showed a smaller enrichment peak as the simulations (25.2 ‰), but the following decline was smaller and slower than the simulated decline.

215 The fine roots (Fig. 1b) observations showed a similar behavior compared to the leaves, with a large increase in  $\delta^{15}\text{N}$  enrichment (45.0 ‰) in during the year of the labeling and some decrease in the first year after labeling (25.5 ‰) then a smooth decline by approximately 50 % over the following decade. The first observed  $\delta^{15}\text{N}$  value in 2007 includes only the upmost layer (0-10 cm), whereas the other observations include fine roots in all the soil layers. The value in the upmost layer is larger than averaged over all the layers, since a lot of fine root biomass is located also at depth 10-20 cm and the  $\delta^{15}\text{N}$   
 220 enrichment decreases with depth. The simulations approximately matched the similar  $\delta^{15}\text{N}$  enrichment peak (value 25.5 ‰) observed in 2008, then showed a faster and larger decline than in the observations, dropping by two-thirds within five years and stabilizing at a lower level of  $\delta^{15}\text{N}$  enrichment compared to the observations.

The observed coarse roots (Fig. 1c) showed a smaller peak in 2007 (30.7 ‰) than fine roots, but had a larger  $\delta^{15}\text{N}$  enrichment peak in 2008 than the leaf and fine root pools. This is suggesting that the tracer was first captured by fine roots and then moved  
 225 into the coarse roots in the following year in the observations. After the peak value of 2008 the observed values declined, levelling off to half of the  $\delta^{15}\text{N}$  peak by 2012. The simulations did not show such a distinct peak, only a small, gradual increase in the first four years (up to 6.6 ‰) and then the  $\delta^{15}\text{N}$  sustained at a steady level, with some slow decrease to level 6.1 ‰, lower than the observations (16.1 ‰).

The observed  $\delta^{15}\text{N}$  in the wood compartment increased by 4.9 ‰ in 2008 compared to the pre-labelled situation and in-  
 230 creased slightly by 2012 (Fig. 1d). The simulations showed a larger  $\delta^{15}\text{N}$  enrichment peak (8.1 ‰), but the peak declined within four years to a level of 2.7 ‰.



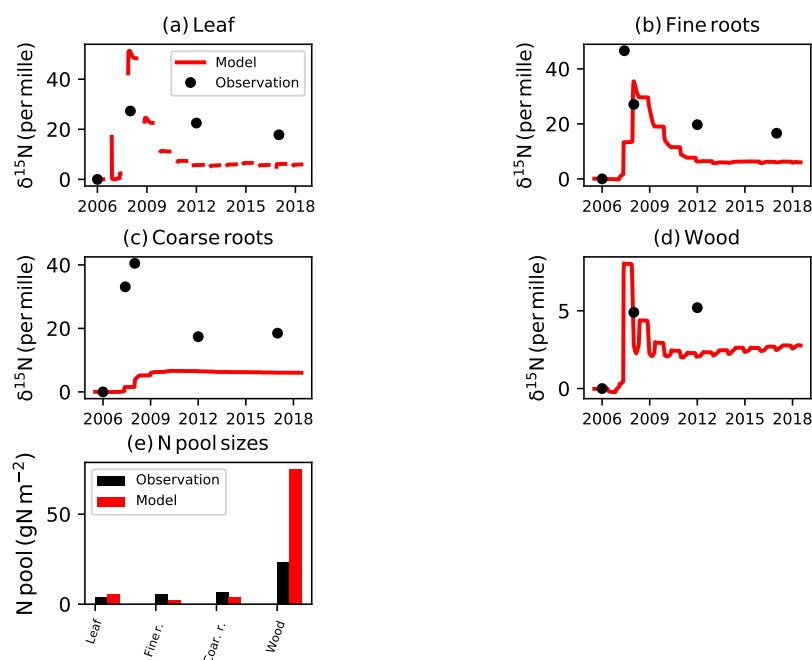


**Figure 1.** The temporal change of the observed (in black) and simulated (in red)  $\delta^{15}\text{N}$  from the reference value in the different vegetation pools (a - leaf, b - fine roots, c - coarse roots, d - heartwood, e - heartwood) and the sizes of the corresponding nitrogen pools (f). Note: The line representing leaf  $\delta^{15}\text{N}$  is not continuous due to the absence of leaves during the dormant season.

The observed soil  $\delta^{15}\text{N}$  signal after 2006 was much larger than the simulated one in all soil pools (Fig. 2), which may partially be the result of the overestimation of the simulated soil N pools in both shallow (3.4-fold overestimated in simulations) and deep soil (2.2-fold overestimated in simulation) (Fig. 3, Table S2). The observations showed a  $\delta^{15}\text{N}$  enrichment peak of 106.4 ‰ in the litter layer compared to the pre-experiment situation and a decrease to about 10.8 ‰ in a decade. In the simulations, the increase in  $\delta^{15}\text{N}$  tracer occurred later and only reached a  $\delta^{15}\text{N}$  enrichment peak of 28.9 ‰ and a decline to a level of 4.6 ‰ in a decade. In the shallow soil layer (0-10 cm), the tracer caused a  $\delta^{15}\text{N}$  enrichment peak of 12.1 ‰ in 2008 and a slow decrease to a level of 15.3 ‰ in a decade. Only an increase of 3.2 ‰ was seen in the simulations and the  $\delta^{15}\text{N}$  enrichment started to slowly decrease, being at the level of 2.7 ‰ after a decade. The deeper soil layers experienced an increase in  $\delta^{15}\text{N}$  by 1.7 ‰ in 2008 and this value slowly increased up to 2.1 ‰ in a decade. The simulations only showed an increase by up to 0.43 ‰ in a decade.

If only soluble litter was considered (Fig. 2a) the fit between simulation (increase in  $\delta^{15}\text{N}$  enrichment peak after labelling now 40.9 ‰) and observation was slightly better. The reason for this discrepancy lies in the immediate "adsorption" of the tracer signals when sprayed to the litter surface, which cannot be represented by the model, since uptake of inorganic N into litter pools is not a flux represented in the model. Instead, the  $\delta^{15}\text{N}$  tracer addition was directly put to the soluble  $\text{NO}_3$  pool,

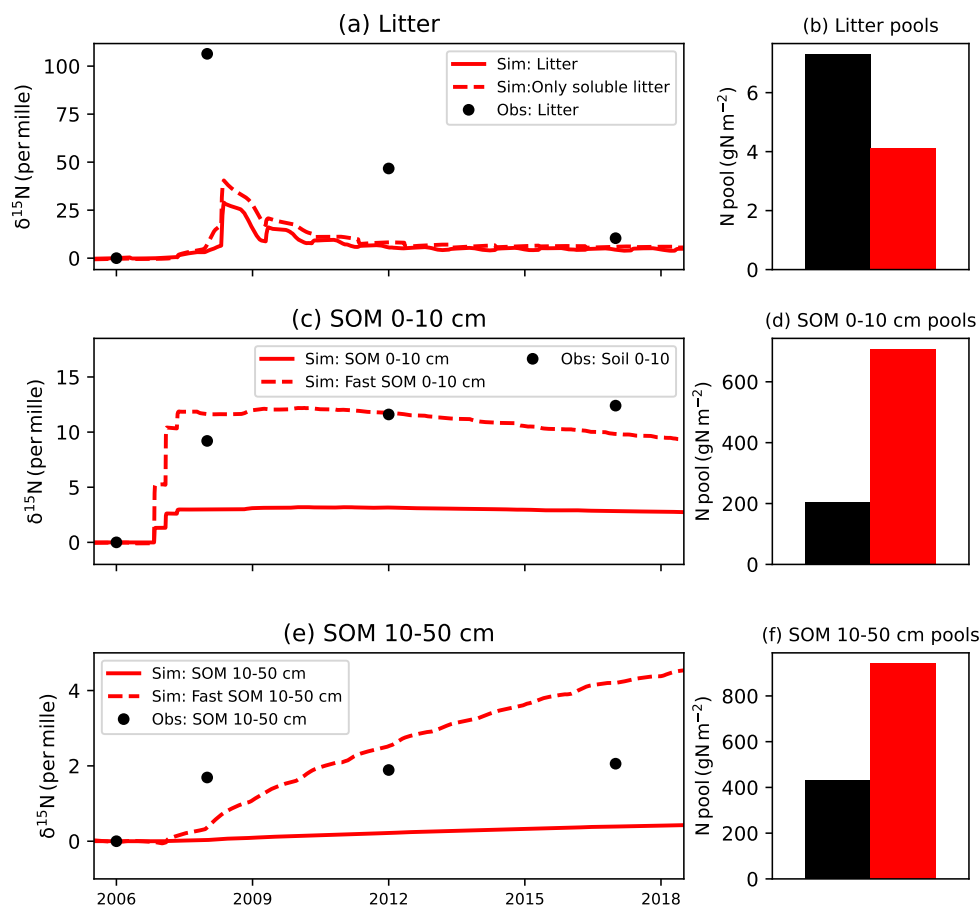


**Figure 2.** The temporal evolution of the observed (in black) and simulated (in red)  $\delta^{15}\text{N}$  signal from the reference value before labeling in the different soil pools (a - litter, c - soil organic matter between 0-10 cm depth, e - soil organic matter between 10-50 cm) and the sizes of the corresponding measured and simulated nitrogen pools (b, d, f). The dashed line shows in a) the soluble litter only, in b) the fast soil pool between 0-10 cm depth and c) the fast soil pool between 10-50 cm.

from where it is subject to plant and microbial uptake, the latter of which generates processes fast SOM, as well as leaching and gaseous emissions. In the simulations, the  $\delta^{15}\text{N}$  signal in the litter was derived only from litter fall of enriched plant material, and thus most of the  $\delta^{15}\text{N}$  tracer addition ended up being immobilised by plants or soil microbes. In fact, while Figures 2b,c show that the model did not capture the magnitude of the bulk SOM  $\delta^{15}\text{N}$  signal, when only considering the fast pool, the observed change in SOM was well captured in the top soil layer (increase in  $\delta^{15}\text{N}$  enrichment peak up to 12.2 ‰) (Fig. 3b). The observed  $\delta^{15}\text{N}$  in the deeper layers did not vary a lot, similar to those changes modelled, although a slight propagation of the surface signal to lower layers can be seen in later years.

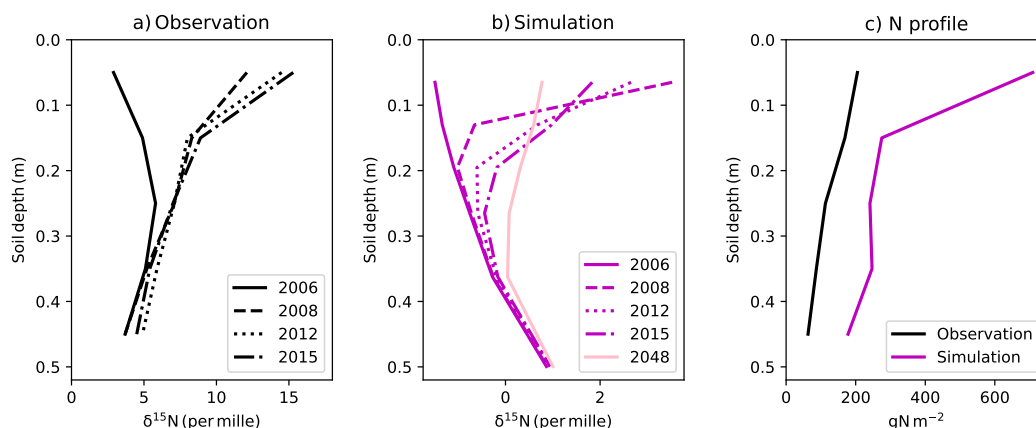


**Figure 3.** The temporal evolution of the observed  $\delta^{15}\text{N}$  at different depths (a) and simulated (b) and the soil profiles of nitrogen in observations and simulations (c).

The development of  $^{15}\text{N}$  tracer at different depths is shown in Fig. 3. The observed soil was more enriched in 2006 than the simulated throughout the depth profile. Also, the observed  $\delta^{15}\text{N}$  signal in the soil was most depleted on top layer, and most enriched at around 0.25 m depth. In the simulations the soil became steadily more enriched towards deeper layers in 2006.

The temporal changes in soil  $\delta^{15}\text{N}$  were much larger in the observations than in the simulations, as was seen already in Fig. 2. In 2008 the increase in observed  $\delta^{15}\text{N}$  was notable already to the depth of 30 cm and then during the coming years, the enrichment continued to increase slowly in the top layers. In the simulations the temporal dynamics were instead different. The top layer was most enriched in 2008 and started depleting afterwards. In 2008 the signal had not yet reached the layers below 20 cm in the simulations and in the following years the enrichment due to the  $\delta^{15}\text{N}$  tracer addition moved to the lower layers gradually. Comparison between the observed and simulated soil N profile showed that the simulations had a large nitrogen pool in the top layer, below which the vertical gradient was more stable and comparable to the observations (Fig. 3).

### 3.3 Recovery of tracer in present day climate and future

Fig. 4 shows the observed and simulated recovery rates of the different vegetation and soil pools. The total amount of recovery was close to 100 % in the simulations. In the observations it was around 70%. Both observations and simulations showed a large fraction of the  $\delta^{15}\text{N}$  signal remaining in the shallow soil layer and the relative contribution from the deeper soil layers was only slowly increasing with time. The observations showed a noticeable fraction of the  $\delta^{15}\text{N}$  signal staying in the litter layer, which was almost depleted by 2017, whereas in the simulations the litter pool did not have a prominent role.

The amount of  $\delta^{15}\text{N}$  signal in coarse roots was pronounced in the observations, but not in the simulation. Both observations and simulation showed a contribution from the fine roots. The simulation showed a contribution from the wood pool already in 2008 by a considerable amount, which remained substantial throughout the years. In the observations the recovery of  $\delta^{15}\text{N}$  to the wood pool occurred in 2008 and increased in 2012 (the wood pool has not been measured in 2017 and we have just

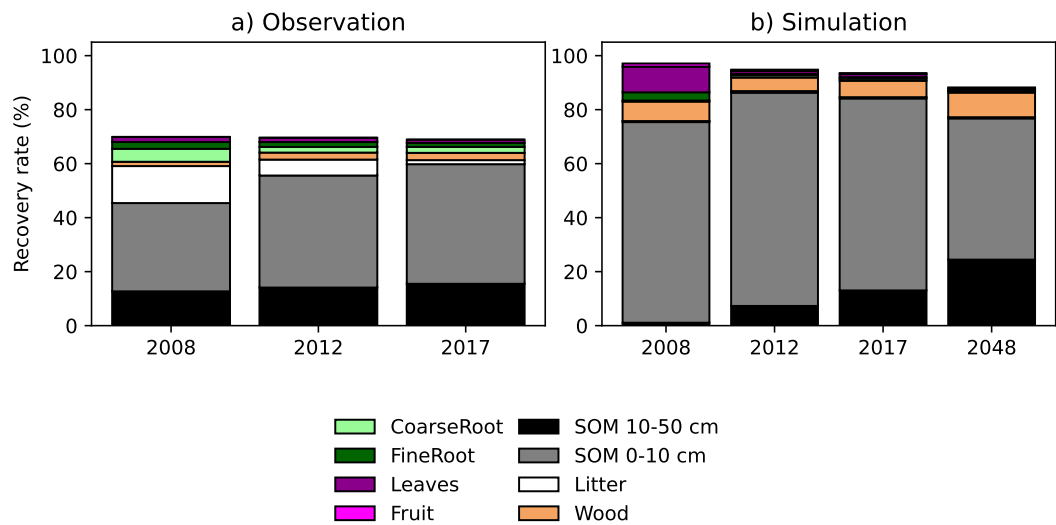


**Figure 4.** The temporal evolution of the observed (a) and simulated (b) recovery rates of different plant and soil pools in different years.

**Table 2.** The recovery rates in the soil and vegetation pools in different years. The observed values are in bold and the simulation results in a regular font. Also the percentual amount of the whole recovered signal in the plants is shown.

Year	2008	2012	2017	2048
Soil	<b>59.1</b> 75.8	<b>61.5</b> 86.9	<b>61.3</b> 84.6	77.2
Plants	<b>10.8</b> 21.3	<b>8.1</b> 7.9	<b>7.6</b> 8.9	11.0
% in plants	<b>15.5</b> 28.1	<b>11.6</b> 9.1	<b>11.0</b> 10.5	14.3

kept its value the same to 2012 in this plot). This difference occurred, partially because we had attributed all of the labile and reserve  $^{15}\text{N}$  to the woody pool, whereas in reality the signal may be mixed between coarse root and woody reserve storage.

275 The simulation showed a large recovery of the  $\delta^{15}\text{N}$  signal in leaves in 2008 (9.5 %), while the observations showed only 1.9 % recovery rate for that year. When considering the separation of soil and plant pools, the observations showed a prominent signal in the soil already in 2008, and its relative contribution was decreasing in the following years (Table 2). The recovery of the label in the plants peaked at 11 % the year after the tracer addition, then stabilized at 8 % at the year 5 and 10. In the simulations, the relative contribution to plants was larger than in the observations in 2008, but close to the observations in 2012

280 and 2017 (Table 2).



**Table 3.** Simulated  $\delta^{15}\text{N}$  recovery in different plant and soil pools in 2017 and 2048.

Pool	2017	2048
Leaf	1.15	0.68
Fine roots	0.53	0.34
Coarse roots	0.79	0.60
Wood	6.09	9.13
Litter	0.46	0.43
Fast SOM (depth 0-50 cm)	71.1	52.3
Slow SOM (depth 0-50 cm)	13.0	24.4

In order to track how much of the  $\delta^{15}\text{N}$  signal remained in the ecosystem over longer timescales, we made a scenario simulation for an additional 30 years. The simulated total recovery rate of the system remained high until the end of the simulation, suggesting a fairly closed simulated nitrogen cycle at the site (Fig. 4b). Most of the signal remained in the soil, with the deeper parts gaining  $\delta^{15}\text{N}$  signal from the top soil layers. The woody pool became more prominent vegetation storage  
 285 for the signal with time.

The vertical profile of simulated  $\delta^{15}\text{N}$  in soil (Fig. 3b) showed that with time it became flatter throughout the soil profile and at the same time the upmost layers got depleted. Table 3 showed the simulated  $\delta^{15}\text{N}$  values of different pools in 2017 and 2048. All other vegetation pools except the wood pool showed a slow decrease in the values during this time period. The  $\delta^{15}\text{N}$  in the litter was slowly decreasing. The  $\delta^{15}\text{N}$  in the fast SOM pool decreased, but increased in the slow SOM pool.

## 290 4 Discussion

### 4.1 Temporal dynamics of the $^{15}\text{N}$ tracer signal

Our simulations showed how the  $^{15}\text{N}$  tracer signal sprayed on the forest floor moved to different ecosystem pools during decennial time scales. Despite some conceptual differences in the description of the manipulation experiment, the QUINCY model successfully simulated many features seen in the observations. The comparison to observations was especially interesting  
 295 when considering the N turnover rates of the vegetation pools. These suggest that the model's turnover rates of N were too fast for the leaves and fine roots. This occurred despite the seemingly higher N retention of leaves during senescence in the model. It is important to note that the model underestimated the C and N pool size of fine roots and C pool size of the leaves, and this might have some influence on the occurring dynamics.

Implementation of nitrate assimilation of soil microorganisms was a key process in order to successfully simulate the tracer  
 300 experiment at the Arnot forest. The natural abundance  $\delta^{15}\text{N}$  in soil differed between the observations and the simulations in 2006, before the start of the experiment, in that observed soil  $\delta^{15}\text{N}$  values were more enriched than in the simulation. Higher



enrichment of soil in the observations would indicate greater losses of N via gaseous pathways which fractionate strongly (Craine et al., 2018; Feng et al., 2023).

Since this is a deciduous forest and the turnover rate of fine roots is set to 0.7 years in the model, it is likely that the  $^{15}\text{N}$  got transferred too quickly away from the compartments that are used to build leaves and fine roots. In the observations the coarse roots showed a large  $^{15}\text{N}$  peak, that was not at all seen in the simulation which showed a gradual increase instead. The model structure did not accommodate a quick response from the coarse roots, that currently have turnover rate of eight years. The observations had larger signal in the coarse roots, because the movement of the signal to the upper tree parts required transport, e.g., via diffusion or xylem transport and additionally the observations of coarse roots include xylem within them (Tegeder and Masclaux-Daubresse, 2018; Van Der Heijden et al., 2015). In QUINCY, we could account for the larger xylem concentration in coarse roots by partitioning the labile and reserve pool between coarse roots, leaves and woody biomass, whereas in this study for simplicity we have assumed they would be allocated in sapwood. Given the simulated peak  $^{15}\text{N}$  signal in labile+reserve pool, partitioning 11 % of the labile+reserve pool to coarse roots would reduce this mismatch. This suggests that the timescale of the transfer of the  $^{15}\text{N}$  signal within the plant (from coarse-roots to woody and leaf compartments), is potentially significantly larger (in the order of months to few years), than the near instantaneous redistribution of nitrogen in the plant as assumed by the model. Finally, it needs to be mentioned that the definition of coarse and fine roots differed slightly between model and observations, as in the observations, roots thicker than 1 mm were considered coarse roots (Goodale, 2017), whereas the threshold was 2 mm in the model.

In the model the tracer was added to top layer of solute  $\text{NO}_3$  which enabled direct access to the plant. The trees were taking up this nitrogen into labile and reserve plant N pools in the model. This caused the plants to have more of the  $^{15}\text{N}$  than the soil in the simulations than observed in the end of 2007, but already in 2008 the plants had relatively more of the signal in the observations than in the simulations. This difference suggests that the simulated plant pools had too high turnover rates for nitrogen, as was also seen separately for the leaves and fine roots compartments. In addition, the strong uptake of the tracer by the litter layer and an ensuing gradual release of  $^{15}\text{N}$  could also have influenced the plant signal in the observations. In the observations the recovery rate in the coarse roots was noticeable still during the last years of the experiment and this supports the fact that the signal was still slowly degrading from the litter and being transported to the plants. Generally the relative recovery of  $^{15}\text{N}$  between plants and soils were comparable between the simulations and the observations in later years. However, during the first years the model estimated nearly double the recovery of  $^{15}\text{N}$  in plants (21 %) than in the observations (11 %), in line with what has been found out in the earlier modeling studies that modeled general N dynamics rather than  $^{15}\text{N}$  cycling (e.g. Cheng et al., 2019).

The observed and measured ecosystem pools differed in their magnitude of N, which also influences the interpretation of  $^{15}\text{N}$  temporal dynamics. These differences were pronounced in the soil, with the modeled total soil N pool ( $1656 \text{ gN m}^{-2}$ ) being more than twice the size that observed ( $744 \text{ gN m}^{-2}$ ). Since in the model the slow soil pool was large, but it was not taking up a lot of the  $^{15}\text{N}$  signal due to its lower turnover rate, its large size caused low values of the  $^{15}\text{N}$  tracer signal. This influence was now shown by representing only the fast pools (Fig. 2), that better captured the observed magnitude changes in the uppermost soil organic matter layer.



In the observations, the  $^{15}\text{N}$  signal occurred in deeper soil layers, down to 0.35 meters, already after one year and at 0.5 m within five years. In the simulation, the downward movement of the  $^{15}\text{N}$  signal was slower. Various factors may contribute to this finding, including a too large uptake of the signal by vegetation and soil biota, a too small movement of  $\text{NO}_3$ , or an underestimation of the transport via bioturbation. Bioturbation in the model is described as simple diffusive flux as in Koven et al. (2013), but with the rate declining with soil depth driven by a decline on the fine root biomass density. This decline might be too strong in QUINCY, but also the amount of C allocation to roots was low-biased in the model, which might have contributed to a too weak bioturbation flux. A further contribution may be that a fraction of the leaching flux was simulated to occur via lateral flow and not deep drainage, effectively partitioning the leaching loss into a lateral component that prevented a fast and deep penetration of the  $^{15}\text{N}$  signal in the soil.

In the observations the top soil layers became more enriched from the incorporation of  $^{15}\text{N}$  from the overlying litter layer, whereas in the simulated top soil was most enriched one year after the tracer application, and then became more depleted as the signal moved deeper to the soil and the vertical soil profile of the  $^{15}\text{N}$  tracer started to get flatter (Fig. 3). These differences between the model results and observations stem from conceptual differences. It is likely that in the observations the  $^{15}\text{N}$  tracer got attached to the litter layer and was being released slowly still after several years, causing continued enrichment to the top soil layer. This is possible in the real world, because the observed litter pool includes early stages of decomposition, typically associated with an increase in N concentration due to immobilisation of mineral N by the decomposers, which facilitates the rapid incorporation of  $^{15}\text{N}$ . In the model, the litter pool only contains fresh litter and any derivatives, including immobilized mineral N, that are partitioned to the fast SOM pool. Disentangling these conceptual differences from any model failure is challenging. It is of note that the considerable overestimation of the soil N pool, that occurred at all depths, was partly influencing the outcome that the soil  $^{15}\text{N}$  signal was more depleted in the model than in the observations.

The  $^{15}\text{N}$  tracer sprayed as  $\text{NO}_3$  remained for a very long time in the soil according to our results for observations and model analysis. This is in line with other natural forest ecosystem  $^{15}\text{N}$  studies (Lin et al., 2024; Templer et al., 2012), where the largest compartment for the recovery was also the soil organic matter. It has been suggested that the  $\text{NO}_3$  would be incorporated to organic matter by abiotic factors (Fitzhugh et al., 2003). These kind of processes are not yet modelled in our current model set-up.

## 4.2 Recovery rates and future

The measurement of recovery rate of the  $^{15}\text{N}$  tracer at the ecosystem scale is very challenging (Craine et al., 2015). The recovery of the signal was close to 100 % in the model throughout the decade after tracer addition, while in the observations, recovery was near 100 % in the days after each tracer addition, but diminished to 77 % by the end of the year the tracer was added, largely due to losses during mid-summer (Goodale et al., 2015). This N was most likely lost via gaseous pathways (denitrification) or via other physical mechanisms, such as leaching. This recovery was quite similar to the average recovery rate of 77.9% for deciduous forests (Templer et al., 2012).

The large difference in total recovery rates between observations and simulation originates from how we describe the  $^{15}\text{N}$  tracer input to the ecosystem in the model. In our simulation the  $^{15}\text{N}$  tracer entered directly to the soluble  $\text{NO}_3$  pool of the





uppermost layer from where it can be taken up by plants or soil microbes, before any gas losses occur. Some gas losses are likely to occur, but since their magnitude cannot be prescribed with certainty, it was not possible to describe this in the model with this approach. Despite the discrepancy in the total recovery rates, we can use our results to investigate how the  $^{15}\text{N}$  is propagating through the different ecosystem compartments.

375 Because of the way we described the tracer experiment in the model, we also did not have a pronounced recovery of the signal in the litter layer, as happened in the observations (Fig. 4). We captured some important characteristics of the observations: a large recovery of the signal in the top soil layers and an increasing recovery of the signal with time in the lower soil layers. The simulation supported a long retention of N in the ecosystem. This was especially visible in the scenario results from year 2048, as the total recovery rate was still staying high (88 %). The movement of the  $^{15}\text{N}$  continued to the lower soil layers  
 380 and the wood became more prominent storage of the  $^{15}\text{N}$  tracer over time, with very low losses of the  $^{15}\text{N}$  tracer from the ecosystem. About 11 % of the recovery was in the plant organs and of this over 80 % in wood (9 % of total recovery). Because of the high C:N ratio in wood, this would imply larger carbon sink compared to N residing in other compartments. For  $\text{NO}_3$  tracer experiments in temperate forests, Lin et al. (2024) found that almost half of the tracer in plants would reside in stem and branches, that would correspond to wood in our simulations, and more than half in roots and leaves. Our results would  
 385 therefore suggest a larger impact on carbon sequestration, but our results span over decadal timescale, that has not been reached in the observations.

### 4.3 Uncertainties in the study

This study has a number of uncertainties. In measurements the heterogeneity and large area of the soil poses a challenge (Templer et al., 2012). In simulation we can capture the overall behaviour based on process understanding. To corroborate,  
 390 whether the issues discovered at Arnot forest are generic model deficits, it would be valuable to extend the analysis to more experiments.

Since our aim was to assess the N retention rates in the ecosystem and the recovery rates in the different ecosystem compartments, we consider our model results to be robust enough for the kind of analysis that we performed. Caldararu et al. (2022) have used Latin hypercube sampling to assess the influence of uncertain fractionation rates for different processes (e.g.  
 395 Robinson, 2001) in the QUINCY model. They found that uncertainties of the fractionation rates did not influence the overall conclusions of their study.

While the QUINCY model covers most fluxes of the terrestrial N cycle, a few processes are missing: it has been long known that some plants are able to use also nitrogen directly from organic material (Näsholm et al., 1998, 2009), and that symbioses with ectomycorrhizae can also support this process (Averill et al., 2014; Chalot and Brun, 1998; Tunlid et al., 2022), but the  
 400 QUINCY model currently does not include these processes. The simulations of this study used the basic soil model (Thum et al., 2019) included in the QUINCY model. To include abovementioned processes it would be better to use as a starting point the more detailed soil model of QUINCY, Jena Soil Model (JSM) (Yu et al., 2020a), which explicitly represents microbial processes and organic matter stabilisation. This new model has been shown to improve the results of soil profile at different sites (Yu et al., 2020a, b) due to microbial process presentation as well as inclusion of organo-mineral association. The organo-



405 mineral association allows to reproduce the soil profile of the C:N ratio better. Including of more processes instead of first-order kinetics descriptions brings the simulation results closer to reality and also simulating this tracer study would benefit from using JSM. Using JSM might also help in more realistic representation of immobilization, that has often been found a caveat in N cycle modelling studies (Cheng et al., 2019).

In the  $^{15}\text{N}$  tracer studies it has also been noticed that the  $^{15}\text{N}$  signal also enters the old wood (G. et al., 2014). This kind of  
410 process is not described in the model and would not be captured. In reality also the canopy is directly taking up N deposition (Ferraretto et al., 2022) and influencing the carbon uptake of vegetation (Li et al., 2025), even though the soil is the most important pathway for the N entering the plants (Craine et al., 2015). In the Arnot forest experiment we simulated the  $^{15}\text{N}$  tracer experiment, where the tracer was sprayed on the forest floor. The application of the tracer on the forest floor allows a lower recovery rate of the tracer than would happen if it was applied on the canopy (Da Ros et al., 2023; Li et al., 2025;  
415 Templer et al., 2012). At the moment we do not have a mechanism in the QUINCY model that would describe the uptake of N deposition via leaves.

## 5 Conclusions

Improving the N cycle in models is of high importance, since the N cycle has a central role in determining the future terrestrial C cycle projections. In this study, we simulated a  $^{15}\text{N}$  tracer experiment conducted at a temperate deciduous forest with the  
420 QUINCY model, which explicitly includes the  $^{15}\text{N}$  cycle. Our results revealed that QUINCY captures the dominant signal from the tracer experiment, the gradual movement of N into the deeper and slower decomposing soil organic material. However, the results also point to a number of model issues, which would not have been obvious from simply comparing the recovery rates with a model that does not track  $^{15}\text{N}$ . The N turnover rates of leaves and fine roots were too fast in the simulations compared against the observations of  $^{15}\text{N}$  temporal dynamics in these pools, suggesting that the vegetation in the model both gains and  
425 loses nitrogen at a faster rate than in real-world ecosystems. We were unable to determine whether this phenomenon was enhanced or even caused by the inability of the model to retain a significant proportion of the  $^{15}\text{N}$  signal in the litter layer. This discrepancy points to a need to re-consider the nitrogen uptake and release in fresh litter. The vertical transport of the  $^{15}\text{N}$  tracer into the soil was also too slow in the simulations. The large amount of soil organic matter in the model likely caused the magnitude of the  $^{15}\text{N}$  tracer signal to be dampened compared to the observations, while considering only the fast, active pool  
430 showed similar behaviour to the observations. This suggests a too large proportion of inert soil organic matter in the model. Because of the way we implemented the  $^{15}\text{N}$  tracer input to the model, we did not capture the initial loss of the tracer signal that occurred in the real-world experiments, but instead had near complete recovery of the tracer signal within the ecosystem close to the tracer input. This recovery was more than a loss of approximately 30 % over the first year in the observations. This value however remained constant after one year. Nevertheless, the recovery rates of plant and soil pools were relatively  
435 comparable between the simulations and the observations after first years, and suggested a gradual accumulation of the added  $^{15}\text{N}$  in the slower soil pools. A simulation run extending up to 2048 showed that the  $^{15}\text{N}$  tracer remained in the ecosystem, with the tracer moving to lower soil depth in the soil and to the woody parts in the vegetation.



**Table A1.** Parameters for the calculation of isotopic fractionation from Robinson (2001).

Symbol	Description	Value	Unit
$R_{ref,C13}$	Reference isotopic mixing ratio of $^{15}\text{N}/^{14}\text{N}$	0.0036765	$\frac{\text{mol}}{\text{mol}}$
$\epsilon_{uptake,NH_4}^{mic}$	Discrimination due to microbial $\text{NH}_4$ uptake	17.0	‰
$\epsilon_{uptake,NO_3}^{mic}$	Discrimination due to microbial $\text{NO}_3$ uptake	13.0	‰
$\epsilon_{uptake,NH_4}^{plant}$	Discrimination due to plant $\text{NH}_4$ uptake	13.5	‰
$\epsilon_{uptake,NO_3}^{plant}$	Discrimination due to plant $\text{NO}_3$ uptake	9.5	‰
$\epsilon_{nit}$	Discrimination due to $\text{N}_2\text{O}$ and $\text{NO}$ production during $\text{NH}_4$ oxidation (nitrification)	47.5	‰
$\epsilon_{nitrate,production}$	Discrimination due to $\text{NO}_3$ production during nitrification	25.0	‰
$\epsilon_{denit}$	Discrimination due to denitrification	31.0	‰
$\epsilon_{ammonification}$	Discrimination due to $\text{NH}_4$ production	2.5	‰

*Code and data availability.* The scientific part of the QUINCY code is available under a GPL v3 license. The source code is available online <https://doi.org/10.17871/quincy-model-2019>), but its access is restricted to registered users. Readers interested in running the model should request a username and password via the Git repository.

The data used in this study, the meteorological forcing to run the model and the model results are available in METIS open data repository (<https://fmi.b2share.csc.fi/records/16d17c16f1d54f60bb52591a03f1a5be>).

## Appendix A

### A1

*Author contributions.* SZ designed the study. TT performed the simulations, analysis and wrote the first draft. CG provided the measured data. Interpretation of results was developed through discussion between all authors. All the authors took part in re-visioning and commenting of the manuscript.

*Competing interests.* The authors declare no competing interests.



450 *Acknowledgements.* TT was supported by the Research Council of Finland (RESEMON project, grant number 330165; and 337552). We thank scientific programmer Dr. Jan Engel for the support with the model maintenance. We thank Prof. Silvia Caldararu for helpful comments to an earlier version of this manuscript.



## References

- Averill, C., Turner, B. L., and Finzi, A. C.: Mycorrhiza-mediated competition between plants and decomposers drives soil carbon storage, *Nature*, 505, 543–545, <https://doi.org/10.1038/nature12901>, <https://www.nature.com/articles/nature12901>, 2014.
- Bonan, G. B.: Ecological climatology: concepts and applications, Cambridge University Press, New York, NY, USA, third edition edn., 2016.
- Buchmann, N., Schulze, E.-D., and Gebauer, G.:  $^{15}\text{N}$ -ammonium and  $^{15}\text{N}$ -nitrate uptake of a 15-year-old *Picea abies* plantation, *Oecologia*, 102, 361–370, <https://doi.org/10.1007/BF00329803>, 1995.
- Butler, T., Marino, R., Schwede, D., Howarth, R., Sparks, J., and Sparks, K.: Atmospheric ammonia measurements at low concentration sites in the northeastern USA: implications for total nitrogen deposition and comparison with CMAQ estimates, *Biogeochemistry*, 122, 191–210, <http://www.jstor.org/stable/24713217>, 2015.
- Caldararu, S., Thum, T., Yu, L., and Zaehle, S.: Whole-plant optimality predicts changes in leaf nitrogen under variable  $\text{CO}_2$  and nutrient availability, *New Phytologist*, 225, 2331–2346, <https://doi.org/10.1111/nph.16327>, <https://onlinelibrary.wiley.com/doi/10.1111/nph.16327>, 2020.
- Caldararu, S., Thum, T., Yu, L., Kern, M., Nair, R., and Zaehle, S.: Long-term ecosystem nitrogen limitation from foliar  $\delta^{15}\text{N}$  data and a land surface model, *Global Change Biology*, 28, 493–508, <https://doi.org/10.1111/gcb.15933>, <https://onlinelibrary.wiley.com/doi/10.1111/gcb.15933>, 2022.
- Canadell, J., Monteiro, P., Costa, M., Cotrim da Cunha, L., Cox, P., Eliseev, A., Henson, S., Ishii, M., Jaccard, S., Koven, C., Lohila, A., Patra, P., Piao, S., Rogelj, J., Syampungani, S., Zaehle, S., and Zickfeld, K.: Global Carbon and other Biogeochemical Cycles and Feedbacks, in: *Climate Change 2021: The Physical Science Basis. Contribution of Working Group I to the Sixth Assessment Report of the Intergovernmental Panel on Climate Change*, edited by Masson-Delmotte, V., Zhai, P., Pirani, A., Connors, S., Péan, C., Berger, S., Caud, N., Chen, Y., Goldfarb, L., Gomis, M., Huang, M., Leitzell, K., Lonnoy, E., Matthews, J., Maycock, T., Waterfield, T., Yelekçi, O., Yu, R., and Zhou, B., Cambridge University Press, Cambridge, UK and New York, NY, USA, <https://doi.org/10.1017/9781009157896.007>, 2022.
- Chalot, M. and Brun, A.: Physiology of organic nitrogen acquisition by ectomycorrhizal fungi and ectomycorrhizas, *FEMS Microbiology Reviews*, 22, 21–44, [https://doi.org/https://doi.org/10.1016/S0168-6445\(98\)00004-7](https://doi.org/https://doi.org/10.1016/S0168-6445(98)00004-7), <https://www.sciencedirect.com/science/article/pii/S0168644598000047>, 1998.
- Cheng, S. J., Hess, P. G., Wieder, W. R., Thomas, R. Q., Nadelhoffer, K. J., Vira, J., Lombardozzi, D. L., Gundersen, P., Fernandez, I. J., Schleppi, P., Gruselle, M.-C., Moldan, F., and Goodale, C. L.: Decadal fates and impacts of nitrogen additions on temperate forest carbon storage: a data–model comparison, *Biogeosciences*, 16, 2771–2793, <https://doi.org/10.5194/bg-16-2771-2019>, <https://bg.copernicus.org/articles/16/2771/2019/>, 2019.
- Craine, J. M., Brookshire, E. N. J., Cramer, M. D., Hasselquist, N. J., Koba, K., Marin-Spiotta, E., and Wang, L.: Ecological interpretations of nitrogen isotope ratios of terrestrial plants and soils, *Plant and Soil*, 396, 1–26, <https://doi.org/10.1007/s11104-015-2542-1>, <http://link.springer.com/10.1007/s11104-015-2542-1>, 2015.
- Craine, J. M., Elmore, A. J., Wang, L., Aranibar, J., Bauters, M., Boeckx, P., Crowley, B. E., Dawes, M. A., Delzon, S., Fajardo, A., Fang, Y., Fujiyoshi, L., Gray, A., Guerrieri, R., Gundale, M. J., Hawke, D. J., Hietz, P., Jonard, M., Kearsley, E., Kenzo, T., Makarov, M., Marañón-Jiménez, S., McGlynn, T. P., McNeil, B. E., Mosher, S. G., Nelson, D. M., Peri, P. L., Roggy, J. C., Sanders-DeMott, R., Song, M., Szpak, P., Templer, P. H., Van der Colff, D., Werner, C., Xu, X., Yang, Y., Yu, G., and Zmudczyńska-Skarbek, K.: Isotopic evidence for oligotrophication of terrestrial ecosystems, *Nature Ecology & Evolution*, 2, 1735–1744, <https://doi.org/10.1038/s41559-018-0694-0>, <http://www.nature.com/articles/s41559-018-0694-0>, 2018.



- 490 Da Ros, L., Rodeghiero, M., Goodale, C. L., Trafoier, G., Panzacchi, P., Giammarchi, F., Tonon, G., and Ventura, M.: Canopy 15N fertilization increases short-term plant N retention compared to ground fertilization in an oak forest, *Forest Ecology and Management*, 539, 121001, <https://doi.org/https://doi.org/10.1016/j.foreco.2023.121001>, <https://www.sciencedirect.com/science/article/pii/S0378112723002359>, 2023.
- de Vries, W., Du, E., and Butterbach-Bahl, K.: Short and long-term impacts of nitrogen deposition on carbon sequestration by forest ecosystems, *Current Opinion in Environmental Sustainability*, 9-10, 90–104, <https://doi.org/https://doi.org/10.1016/j.cosust.2014.09.001>, <https://www.sciencedirect.com/science/article/pii/S1877343514000566>, sI: System dynamics and sustainability, 2014.
- 495 Du, E. and de Vries, W.: Nitrogen-induced new net primary production and carbon sequestration in global forests, *Environmental Pollution*, 242, 1476–1487, <https://doi.org/https://doi.org/10.1016/j.envpol.2018.08.041>, <https://www.sciencedirect.com/science/article/pii/S0269749118325090>, 2018.
- 500 Fahey, T. J., Yavitt, J. B., Sherman, R. E., Maerz, J. C., Groffman, P. M., Fisk, M. C., and Bohlen, P. J.: Earthworm effects on the incorporation of litter C and N into soil organic matter in a sugar maple forest, *Ecological Applications*, 23, 1185–1201, <https://doi.org/https://doi.org/10.1890/12-1760.1>, <https://esajournals.onlinelibrary.wiley.com/doi/abs/10.1890/12-1760.1>, 2013.
- Fain, J. J., Volk, T. A., and Fahey, T. J.: Fifty Years of Change in an Upland Forest in South-Central New York: General Patterns, *Bulletin of the Torrey Botanical Club*, 121, 130–139, <http://www.jstor.org/stable/2997164>, 1994.
- 505 Feng, M., Peng, S., Wang, Y., Ciais, P., Goll, D. S., Chang, J., Fang, Y., Houlton, B. Z., Liu, G., Sun, Y., and Xi, Y.: Overestimated nitrogen loss from denitrification for natural terrestrial ecosystems in CMIP6 Earth System Models, *Nature Communications*, 14, 3065, <https://doi.org/10.1038/s41467-023-38803-z>, <https://www.nature.com/articles/s41467-023-38803-z>, 2023.
- Ferraretto, D., Nair, R., Shah, N. W., Reay, D., Mencuccini, M., Spencer, M., and Heal, K. V.: Forest canopy nitrogen uptake can supply entire foliar demand, *Functional Ecology*, 36, 933–949, <https://doi.org/https://doi.org/10.1111/1365-2435.14005>, <https://besjournals.onlinelibrary.wiley.com/doi/abs/10.1111/1365-2435.14005>, 2022.
- 510 Fitzhugh, R. D., Lovett, G. M., and Venterea, R. T.: Biotic and abiotic immobilization of ammonium, nitrite, and nitrate in soils developed under different tree species in the Catskill Mountains, New York, USA, *Global Change Biology*, 9, 1591–1601, <https://doi.org/https://doi.org/10.1046/j.1365-2486.2003.00694.x>, <https://onlinelibrary.wiley.com/doi/abs/10.1046/j.1365-2486.2003.00694.x>, 2003.
- 515 Fleischer, K., Dolman, A. J., van der Molen, M. K., Rebel, K. T., Erisman, J. W., Wassen, M. J., Pak, B., Lu, X., Rammig, A., and Wang, Y.-P.: Nitrogen Deposition Maintains a Positive Effect on Terrestrial Carbon Sequestration in the 21st Century Despite Growing Phosphorus Limitation at Regional Scales, *Global Biogeochemical Cycles*, 33, 810–824, <https://doi.org/https://doi.org/10.1029/2018GB005952>, <https://agupubs.onlinelibrary.wiley.com/doi/abs/10.1029/2018GB005952>, 2019.
- Friedlingstein, P., O'Sullivan, M., Jones, M. W., Andrew, R. M., Hauck, J., Landschützer, P., Le Quéré, C., Li, H., Luijckx, I. T., Olsen, A., Peters, G. P., Peters, W., Pongratz, J., Schwingshackl, C., Sitch, S., Canadell, J. G., Ciais, P., Jackson, R. B., Alin, S. R., Arneth, A., Arora, V., Bates, N. R., Becker, M., Bellouin, N., Berghoff, C. F., Bittig, H. C., Bopp, L., Cadule, P., Campbell, K., Chamberlain, M. A., Chandra, N., Chevallier, F., Chini, L. P., Colligan, T., Decayeux, J., Djeutchouang, L. M., Dou, X., Duran Rojas, C., Enyo, K., Evans, W., Fay, A. R., Feely, R. A., Ford, D. J., Foster, A., Gasser, T., Gehlen, M., Gkritzalis, T., Grassi, G., Gregor, L., Gruber, N., Gürses, O., Harris, I., Hefner, M., Heinke, J., Hurtt, G. C., Iida, Y., Ilyina, T., Jacobson, A. R., Jain, A. K., Jarníková, T., Jersild, A., Jiang, F., Jin, Z., Kato, E., Keeling, R. F., Klein Goldewijk, K., Knauer, J., Korsbakken, J. I., Lan, X., Lauvset, S. K., Lefèvre, N., Liu, Z., Liu, J., Ma, L., Maksyutov, S., Marland, G., Mayot, N., McGuire, P. C., Metzl, N., Monacchi, N. M., Morgan, E. J., Nakaoka, S.-I., Neill, C., Niwa, Y., Nützel, T., Olivier, L., Ono, T., Palmer, P. I., Pierrot, D., Qin, Z., Resplandy, L., Roobaert, A., Rosan, T. M., Rödenbeck, C., Schwinger,
- 525



- J., Smallman, T. L., Smith, S. M., Sospedra-Alfonso, R., Steinhoff, T., Sun, Q., Sutton, A. J., Séférián, R., Takao, S., Tatebe, H., Tian, H., Tilbrook, B., Torres, O., Tourigny, E., Tsujino, H., Tubiello, F., van der Werf, G., Wanninkhof, R., Wang, X., Yang, D., Yang, X., Yu, Z., Yuan, W., Yue, X., Zaehle, S., Zeng, N., and Zeng, J.: Global Carbon Budget 2024, *Earth System Science Data*, 17, 965–1039, <https://doi.org/10.5194/essd-17-965-2025>, <https://essd.copernicus.org/articles/17/965/2025/>, 2025.
- Friend, A. D., Stevens, A. K., Knox, R. G., and Cannell, M. G. R.: A process-based, terrestrial biosphere model of ecosystem dynamics (Hybrid v3.0), *Ecological modelling*, 95, 249–287, 1997.
- G., T., W., S. R. T., N., B., P., S., P., W., and P., W.: The mobility of nitrogen across tree-rings of Norway spruce (*Picea abies* L.) and the effect of extraction method on tree-ring  $\delta^{15}\text{N}$  and  $\delta^{13}\text{C}$  values, *Rapid Communications in Mass Spectrometry*, 28, 1258–1264, <https://doi.org/https://doi.org/10.1002/rcm.6897>, <https://analyticalsciencejournals.onlinelibrary.wiley.com/doi/abs/10.1002/rcm.6897>, 2014.
- Galloway, J. N., Townsend, A. R., Erisman, J. W., Bekunda, M., Cai, Z., Freney, J. R., Martinelli, L. A., Seitzinger, S. P., and Sutton, M. A.: Transformation of the Nitrogen Cycle: Recent Trends, Questions, and Potential Solutions, *Science*, 320, 889–892, <https://doi.org/10.1126/science.1136674>, <https://www.science.org/doi/10.1126/science.1136674>, 2008.
- Gong, C., Tian, H., Liao, H., Pan, N., Pan, S., Ito, A., Jain, A. K., Kou-Giesbrecht, S., Joos, F., Sun, Q., Shi, H., Vuichard, N., Zhu, Q., Peng, C., Maggi, F., Tang, F. H. M., and Zaehle, S.: Global net climate effects of anthropogenic reactive nitrogen, *Nature*, 632, 557–563, <https://doi.org/10.1038/s41586-024-07714-4>, <https://www.nature.com/articles/s41586-024-07714-4>, 2024.
- Goodale, C. L.: Multiyear fate of a  $^{15}\text{N}$  tracer in a mixed deciduous forest: retention, redistribution, and differences by mycorrhizal association, *Global Change Biology*, 23, 867–880, <https://doi.org/10.1111/gcb.13483>, <http://doi.wiley.com/10.1111/gcb.13483>, 2017.
- Goodale, C. L., Fredriksen, G., Weiss, M. S., McCalley, C. K., Sparks, J. P., and Thomas, S. A.: Soil processes drive seasonal variation in retention of  $^{15}\text{N}$  tracers in a deciduous forest catchment, *Ecology*, 96, 2653–2668, <https://doi.org/10.1890/14-1852.1>, <http://doi.wiley.com/10.1890/14-1852.1>, 2015.
- Gruber, N. and Galloway, J. N.: An Earth-system perspective of the global nitrogen cycle, *Nature*, 451, 293–296, <https://doi.org/10.1038/nature06592>, <http://www.nature.com/articles/nature06592>, 2008.
- Gurmesa, G. A., Wang, A., Li, S., Peng, S., De Vries, W., Gundersen, P., Ciais, P., Phillips, O. L., Hobbie, E. A., Zhu, W., Nadelhoffer, K., Xi, Y., Bai, E., Sun, T., Chen, D., Zhou, W., Zhang, Y., Guo, Y., Zhu, J., Duan, L., Li, D., Koba, K., Du, E., Zhou, G., Han, X., Han, S., and Fang, Y.: Retention of deposited ammonium and nitrate and its impact on the global forest carbon sink, *Nature Communications*, 13, 880, <https://doi.org/10.1038/s41467-022-28345-1>, <https://www.nature.com/articles/s41467-022-28345-1>, 2022.
- Hyvönen, R., Persson, T., Andersson, S., Olsson, B., Ågren, G. I., and Linder, S.: Impact of Long-Term Nitrogen Addition on Carbon Stocks in Trees and Soils in Northern Europe, *Biogeochemistry*, 89, 121–137, <http://www.jstor.org/stable/40343590>, 2008.
- Högberg, P., Näsholm, T., Franklin, O., and Högberg, M. N.: Tamm Review: On the nature of the nitrogen limitation to plant growth in Fennoscandian boreal forests, *Forest Ecology and Management*, 403, 161–185, <https://doi.org/https://doi.org/10.1016/j.foreco.2017.04.045>, <https://www.sciencedirect.com/science/article/pii/S0378112717300191>, 2017.
- Jain, A., Yang, X., Khashgi, H., McGuire, A. D., Post, W., and Kicklighter, D.: Nitrogen attenuation of terrestrial carbon cycle response to global environmental factors, *Global Biogeochemical Cycles*, 23, <https://doi.org/https://doi.org/10.1029/2009GB003519>, <https://agupubs.onlinelibrary.wiley.com/doi/abs/10.1029/2009GB003519>, 2009.





- Koven, C. D., Riley, W. J., Subin, Z. M., Tang, J. Y., Torn, M. S., Collins, W. D., Bonan, G. B., Lawrence, D. M., and Swenson, S. C.:  
 565 The effect of vertically resolved soil biogeochemistry and alternate soil C and N models on C dynamics of CLM4, *Biogeosciences*, 10,  
 7109–7131, <https://doi.org/10.5194/bg-10-7109-2013>, <https://bg.copernicus.org/articles/10/7109/2013/>, 2013.
- Kull, O. and Kruijt, B.: Leaf photosynthetic light response: a mechanistic model for scaling photosynthesis to leaves and canopies, *Functional Ecology*, 12, 767–777, 1998.
- Lamarque, J.-F., Bond, T. C., Eyring, V., Granier, C., Heil, A., Klimont, Z., Lee, D., Liousse, C., Mieville, A., Owen, B., Schultz, M. G.,  
 570 Shindell, D., Smith, S. J., Stehfest, E., Van Aardenne, J., Cooper, O. R., Kainuma, M., Mahowald, N., McConnell, J. R., Naik, V.,  
 Riahi, K., and van Vuuren, D. P.: Historical (1850–2000) gridded anthropogenic and biomass burning emissions of reactive gases and  
 aerosols: methodology and application, *Atmospheric Chemistry and Physics*, 10, 7017–7039, <https://doi.org/10.5194/acp-10-7017-2010>,  
<https://www.atmos-chem-phys.net/10/7017/2010/>, 2010.
- Lamarque, J.-F., Kyle, G. P., Meinshausen, M., Riahi, K., Smith, S. J., van Vuuren, D. P., Conley, A. J., and Vitt, F.: Global and regional  
 575 evolution of short-lived radiatively-active gases and aerosols in the Representative Concentration Pathways, *Climatic Change*, 109, 191,  
<https://doi.org/10.1007/s10584-011-0155-0>, <https://doi.org/10.1007/s10584-011-0155-0>, 2011.
- Le Quéré, C., Andrew, R. M., Friedlingstein, P., Sitch, S., Pongratz, J., Manning, A. C., Korsbakken, J. I., Peters, G. P., Canadell, J. G.,  
 Jackson, R. B., Boden, T. A., Tans, P. P., Andrews, O. D., Arora, V. K., Bakker, D. C. E., Barbero, L., Becker, M., Betts, R. A., Bopp,  
 L., Chevallier, F., Chini, L. P., Ciais, P., Cosca, C. E., Cross, J., Currie, K., Gasser, T., Harris, I., Hauck, J., Haverd, V., Houghton, R. A.,  
 580 Hunt, C. W., Hurtt, G., Ilyina, T., Jain, A. K., Kato, E., Kautz, M., Keeling, R. F., Klein Goldewijk, K., Körtzinger, A., Landschützer, P.,  
 Lefèvre, N., Lenton, A., Lienert, S., Lima, I., Lombardozzi, D., Metzl, N., Millero, F., Monteiro, P. M. S., Munro, D. R., Nabel, J. E. M. S.,  
 Nakaoka, S.-I., Nojiri, Y., Padin, X. A., Pregon, A., Pfeil, B., Pierrot, D., Poulter, B., Rehder, G., Reimer, J., Rödenbeck, C., Schwinger,  
 J., Séférian, R., Skjelvan, I., Stocker, B. D., Tian, H., Tilbrook, B., Tubiello, F. N., van der Laan-Luijckx, I. T., van der Werf, G. R., van  
 Heuven, S., Viovy, N., Vuichard, N., Walker, A. P., Watson, A. J., Wiltshire, A. J., Zaehle, S., and Zhu, D.: Global Carbon Budget 2017,  
 585 *Earth System Science Data*, 10, 405–448, <https://doi.org/10.5194/essd-10-405-2018>, <https://www.earth-syst-sci-data.net/10/405/2018/>,  
 2018.
- LeBauer, D. S. and Treseder, K. K.: Nitrogen Limitation Of Net Primary Productivity In Terrestrial Ecosystems Is Globally Distributed,  
*Ecology*, 89, 371–379, <https://doi.org/10.1890/06-2057.1>, <http://doi.wiley.com/10.1890/06-2057.1>, 2008.
- Li, X., Zhang, C., Zhang, B., Jiang, L., Tang, S., Sun, C., Bai, Y., Wang, Y., Shi, Y., Ma, L., Zhang, W., Ye, Q., Yan, J., Wang,  
 590 K., Fu, J., Du, W., Ha, D., Ju, Y., Wan, S., Hong, L., Fang, Y., Siemann, E., Luo, Y., Reich, P. B., and Fu, S.: Underappreciated  
 role of canopy nitrogen deposition for forest productivity, *Proceedings of the National Academy of Sciences*, 122, e2508925122,  
<https://doi.org/10.1073/pnas.2508925122>, <https://www.pnas.org/doi/abs/10.1073/pnas.2508925122>, 2025.
- Lin, Q., Zhu, J., Wang, Q., Zhang, Q., and Yu, G.: Patterns and drivers of atmospheric nitrogen deposition retention in global forests,  
*Global Change Biology*, 30, e17410, <https://doi.org/https://doi.org/10.1111/gcb.17410>, <https://onlinelibrary.wiley.com/doi/abs/10.1111/gcb.17410>,  
 595 e17410 GCB-24-1032.R1, 2024.
- Magnani, F., Mencuccini, M., Borghetti, M., Berbigier, P., Berninger, F., Delzon, S., Grelle, A., Hari, P., Jarvis, P. G., Kolari, P.,  
 Kowalski, A. S., Lankreijer, H., Law, B. E., Lindroth, A., Loustau, D., Manca, G., Moncrieff, J. B., Rayment, M., Tedeschi, V.,  
 Valentini, R., and Grace, J.: The human footprint in the carbon cycle of temperate and boreal forests, *Nature*, 447, 849–851,  
<https://doi.org/10.1038/nature05847>, <http://www.nature.com/articles/nature05847>, 2007.



- 600 Meyerholt, J. and Zaehle, S.: The role of stoichiometric flexibility in modelling forest ecosystem responses to nitrogen fertilization, *New Phytologist*, 208, 1042–1055, <https://doi.org/https://doi.org/10.1111/nph.13547>, <https://nph.onlinelibrary.wiley.com/doi/abs/10.1111/nph.13547>, 2015.
- Meyerholt, J., Zaehle, S., and Smith, M. J.: Variability of projected terrestrial biosphere responses to elevated levels of atmospheric CO<sub>2</sub> due to uncertainty in biological nitrogen fixation, *Biogeosciences*, 13, 1491–1518, <https://doi.org/10.5194/bg-13-1491-2016>, <https://www.biogeosciences.net/13/1491/2016/>, 2016.
- 605 Meyerholt, J., Sickel, K., and Zaehle, S.: Ensemble projections elucidate effects of uncertainty in terrestrial nitrogen limitation on future carbon uptake, *Global Change Biology*, 26, 3978–3996, <https://doi.org/https://doi.org/10.1111/gcb.15114>, <https://onlinelibrary.wiley.com/doi/abs/10.1111/gcb.15114>, 2020.
- Nadelhoffer, K., Downs, M., Fry, B., Magill, A., and Aber, J.: Controls on N Retention and Exports in a Forested Watershed, *Environmental Monitoring and Assessment*, 55, 187–210, <https://doi.org/10.1023/A:1006190222768>, 1999a.
- 610 Nadelhoffer, K. J., Emmett, B. A., Gundersen, P., Kjønnaas, O. J., Koopmans, C. J., Schleppi, P., Tietema, A., and Wright, R. F.: Nitrogen deposition makes a minor contribution to carbon sequestration in temperate forests, *Nature*, 398, 145–148, <https://doi.org/10.1038/18205>, <https://www.nature.com/articles/18205>, 1999b.
- Näsholm, T., Ekblad, A., Nordin, A., Giesler, R., Högberg, M., and Högberg, P.: Boreal forest plants take up organic nitrogen, *Nature*, 392, 914–916, <https://doi.org/10.1038/31921>, <http://www.nature.com/articles/31921>, 1998.
- 615 Näsholm, T., Kielland, K., and Ganeteg, U.: Uptake of organic nitrogen by plants, *New Phytologist*, 182, 31–48, <https://doi.org/https://doi.org/10.1111/j.1469-8137.2008.02751.x>, <https://nph.onlinelibrary.wiley.com/doi/abs/10.1111/j.1469-8137.2008.02751.x>, 2009.
- Parton, W. J., Scurlock, J. M. O., Ojima, D. S., Gilmanov, T. G., Scholes, R. J., Schimmel, D. S., Kirchner, T., Menaut, J. C., Seastedt, T., Moya, E. G., Kamnalrut, A., and Kinyamario, J. I.: Observations and modelling of biomass and soil organic matter dynamics for the grassland biome worldwide, *Global Biogeochemical Cycles*, 7, 785–809, 1993.
- 620 Quinn Thomas, R., Canham, C. D., Weathers, K. C., and Goodale, C. L.: Increased tree carbon storage in response to nitrogen deposition in the US, *Nature Geoscience*, 3, 13–17, <https://doi.org/10.1038/ngeo721>, <http://www.nature.com/articles/ngeo721>, 2010.
- Reay, D. S., Dentener, F., Smith, P., Grace, J., and Feely, R. A.: Global nitrogen deposition and carbon sinks, *Nature Geoscience*, 1, 430–437, <https://doi.org/10.1038/ngeo230>, <http://www.nature.com/articles/ngeo230>, 2008.
- 625 Riahi, K., Rao, S., Krey, V., Cho, C., Chirkov, V., Fischer, G., Kindermann, G., Nakicenovic, N., and Rafaj, P.: RCP 8.5—A scenario of comparatively high greenhouse gas emissions, *Climatic Change*, 109, 33–57, <https://doi.org/10.1007/s10584-011-0149-y>, <http://link.springer.com/10.1007/s10584-011-0149-y>, 2011.
- Robinson, D.:  $\delta^{15}\text{N}$  as an integrator of the nitrogen cycle, *Trends in Ecology & Evolution*, 16, 153–162, [https://doi.org/10.1016/S0169-5347\(00\)02098-X](https://doi.org/10.1016/S0169-5347(00)02098-X), <https://linkinghub.elsevier.com/retrieve/pii/S016953470002098X>, 2001.
- 630 Rogers, A., Medlyn, B. E., Dukes, J. S., Bonan, G., von Caemmerer, S., Dietze, M. C., Kattge, J., Leakey, A. D. B., Mercado, L. M., Niinemets, U. U., Prentice, I. C., Serbin, S. P., Sitch, S., Way, D. A., and Zaehle, S.: A roadmap for improving the representation of photosynthesis in Earth system models, *New Phytologist*, 213, 22–42, <https://doi.org/https://doi.org/10.1111/nph.14283>, <https://nph.onlinelibrary.wiley.com/doi/abs/10.1111/nph.14283>, 2017.
- 635 Schleppi, P. and Wessel, W. W.: Experimental Design and Interpretation of Terrestrial Ecosystem Studies Using <sup>15</sup>N Tracers: Practical and Statistical Considerations, *Frontiers in Environmental Science*, 9, 174, <https://doi.org/10.3389/fenvs.2021.658779>, <https://www.frontiersin.org/article/10.3389/fenvs.2021.658779>, 2021.



- Schlesinger, W. H.: On the fate of anthropogenic nitrogen, *Proceedings of the National Academy of Sciences*, 106, 203–208, <https://doi.org/10.1073/pnas.0810193105>, <https://pnas.org/doi/full/10.1073/pnas.0810193105>, 2009.
- 640 Schulte-Uebbing, L. and de Vries, W.: Global-scale impacts of nitrogen deposition on tree carbon sequestration in tropical, temperate, and boreal forests: A meta-analysis, *Global Change Biology*, 24, e416–e431, <https://doi.org/https://doi.org/10.1111/gcb.13862>, <https://onlinelibrary.wiley.com/doi/abs/10.1111/gcb.13862>, 2018.
- Schulte-Uebbing, L. F., Ros, G. H., and de Vries, W.: Experimental evidence shows minor contribution of nitrogen deposition to global forest carbon sequestration, *Global Change Biology*, 28, 899–917, <https://doi.org/https://doi.org/10.1111/gcb.15960>, <https://onlinelibrary.wiley.com/doi/abs/10.1111/gcb.15960>, 2022.
- 645 Seiler, C., Melton, J. R., Arora, V. K., Sitch, S., Friedlingstein, P., Anthoni, P., Goll, D., Jain, A. K., Joetzjer, E., Lienert, S., Lombardozzi, D., Luyssaert, S., Nabel, J. E. M. S., Tian, H., Vuichard, N., Walker, A. P., Yuan, W., and Zaehle, S.: Are Terrestrial Biosphere Models Fit for Simulating the Global Land Carbon Sink?, *Journal of Advances in Modeling Earth Systems*, 14, e2021MS002946, <https://doi.org/https://doi.org/10.1029/2021MS002946>, <https://agupubs.onlinelibrary.wiley.com/doi/abs/10.1029/2021MS002946>, e2021MS002946 2021MS002946, 2022.
- 650 Sutton, M. A., Simpson, D., Levy, P. E., Smith, R. I., Reis, S., Van OIJEN, M., and De VRIES, W.: Uncertainties in the relationship between atmospheric nitrogen deposition and forest carbon sequestration: nitrogen and forest carbon sequestration, *Global Change Biology*, 14, 2057–2063, <https://doi.org/10.1111/j.1365-2486.2008.01636.x>, <https://onlinelibrary.wiley.com/doi/10.1111/j.1365-2486.2008.01636.x>, 2008.
- 655 Tegeder, M. and Masclaux-Daubresse, C.: Source and sink mechanisms of nitrogen transport and use, *New Phytologist*, 217, 35–53, <https://doi.org/https://doi.org/10.1111/nph.14876>, <https://nph.onlinelibrary.wiley.com/doi/abs/10.1111/nph.14876>, 2018.
- Templer, P. H., Mack, M. C., Iii, F. S. C., Christenson, L. M., Compton, J. E., Crook, H. D., Currie, W. S., Curtis, C. J., Dail, D. B., D'Antonio, C. M., Emmett, B. A., Epstein, H. E., Goodale, C. L., Gundersen, P., Hobbie, S. E., Holland, K., Hooper, D. U., Hungate, B. A., Lamontagne, S., Nadelhoffer, K. J., Osenberg, C. W., Perakis, S. S., Schleppei, P., Schimel, J., Schmidt, I. K., Sommerkorn, M., 660 Spoelstra, J., Tietema, A., Wessel, W. W., and Zak, D. R.: Sinks for nitrogen inputs in terrestrial ecosystems: a meta-analysis of <sup>15</sup>N tracer field studies, *Ecology*, 93, 1816–1829, <https://doi.org/10.1890/11-1146.1>, <http://doi.wiley.com/10.1890/11-1146.1>, 2012.
- Thomas, R. Q., Zaehle, S., Templer, P. H., and Goodale, C. L.: Global patterns of nitrogen limitation: confronting two global biogeochemical models with observations, *Global Change Biology*, 19, 2986–2998, <https://doi.org/https://doi.org/10.1111/gcb.12281>, <https://onlinelibrary.wiley.com/doi/abs/10.1111/gcb.12281>, 2013.
- 665 Thomas, R. Q., Brookshire, E. N. J., and Gerber, S.: Nitrogen limitation on land: how can it occur in Earth system models?, *Global Change Biology*, 21, 1777–1793, <https://doi.org/10.1111/gcb.12813>, <https://onlinelibrary.wiley.com/doi/10.1111/gcb.12813>, 2015.
- Thum, T., Caldararu, S., Engel, J., Kern, M., Pallandt, M., Schnur, R., Yu, L., and Zaehle, S.: A new model of the coupled carbon, nitrogen, and phosphorus cycles in the terrestrial biosphere (QUINCY v1.0; revision 1996), *Geoscientific Model Development*, 12, 4781–4802, <https://doi.org/10.5194/gmd-12-4781-2019>, <https://gmd.copernicus.org/articles/12/4781/2019/>, 2019.
- 670 Tunlid, A., Floudas, D., Op De Beeck, M., Wang, T., and Persson, P.: Decomposition of soil organic matter by ectomycorrhizal fungi: Mechanisms and consequences for organic nitrogen uptake and soil carbon stabilization, *Frontiers in Forests and Global Change*, Volume 5 - 2022, <https://doi.org/10.3389/ffgc.2022.934409>, <https://www.frontiersin.org/journals/forests-and-global-change/articles/10.3389/ffgc.2022.934409>, 2022.



- University of East Anglia Climatic Research Unit, Harris, I.: CRU JRA v2.1: A forcings dataset of gridded land surface blend of Climatic  
 675 Research Unit (CRU) and Japanese reanalysis (JRA) data; Jan.1901 - Dec.2019. Centre for Environmental Data Analysis, <https://catalogue.ceda.ac.uk/uuid/10d2c73e5a7d46f4ada08b0a26302ef7>, last accessed 9 June 2021, 2020.
- Van Der Heijden, G., Dambrine, E., Pollier, B., Zeller, B., Ranger, J., and Legout, A.: Mg and Ca uptake by roots in relation to depth and allocation to aboveground tissues: results from an isotopic labeling study in a beech forest on base-poor soil, *Biogeochemistry*, 122, 375–393, <https://doi.org/10.1007/s10533-014-0047-2>, <http://link.springer.com/10.1007/s10533-014-0047-2>, 2015.
- 680 Van Houtven, G., Phelan, J., Clark, C., Sabo, R. D., Buckley, J., Thomas, R. Q., Horn, K., and LeDuc, S. D.: Nitrogen deposition and climate change effects on tree species composition and ecosystem services for a forest cohort, *Ecological Monographs*, 89, e01345, <https://doi.org/https://doi.org/10.1002/ecm.1345>, <https://esajournals.onlinelibrary.wiley.com/doi/abs/10.1002/ecm.1345>, 2019.
- Vicca, S., Stocker, B. D., Reed, S., Wieder, W. R., Bahn, M., Fay, P. A., Janssens, I. A., Lambers, H., Peñuelas, J., Piao, S., Rebel, K. T., Sardans, J., Sigurdsson, B. D., Van Sundert, K., Wang, Y.-P., Zaehle, S., and Ciais, P.: Using research networks to create the comprehensive  
 685 datasets needed to assess nutrient availability as a key determinant of terrestrial carbon cycling, *Environmental Research Letters*, 13, 125006, <https://doi.org/10.1088/1748-9326/aaeae7>, <https://iopscience.iop.org/article/10.1088/1748-9326/aaeae7>, 2018.
- Wang, R., Goll, D., Balkanski, Y., Hauglustaine, D., Boucher, O., Ciais, P., Janssens, I., Penuelas, J., Guenet, B., Sardans, J., Bopp, L., Vuichard, N., Zhou, F., Li, B., Piao, S., Peng, S., Huang, Y., and Tao, S.: Global forest carbon uptake due to nitrogen and phosphorus deposition from 1850 to 2100, *Global Change Biology*, 23, 4854–4872, <https://doi.org/https://doi.org/10.1111/gcb.13766>,  
 690 <https://onlinelibrary.wiley.com/doi/abs/10.1111/gcb.13766>, 2017.
- Yu, L., Ahrens, B., Wutzler, T., Schrumpf, M., and Zaehle, S.: Jena Soil Model (JSM v1.0; revision 1934): a microbial soil organic carbon model integrated with nitrogen and phosphorus processes, *Geoscientific Model Development*, 13, 783–803, <https://doi.org/10.5194/gmd-13-783-2020>, <https://gmd.copernicus.org/articles/13/783/2020/>, 2020a.
- Yu, L., Ahrens, B., Wutzler, T., Zaehle, S., and Schrumpf, M.: Modeling Soil Responses to Nitrogen and Phosphorus Fertilization Along a  
 695 Soil Phosphorus Stock Gradient, *Frontiers in Forests and Global Change*, 3, 118, <https://doi.org/10.3389/ffgc.2020.543112>, <https://www.frontiersin.org/article/10.3389/ffgc.2020.543112>, 2020b.
- Zaehle, S. and Dalmonech, D.: Carbon–nitrogen interactions on land at global scales: current understanding in modelling climate biosphere feedbacks, *Current Opinion in Environmental Sustainability*, 3, 311–320, 2011.
- Zaehle, S. and Friend, A. D.: Carbon and nitrogen cycle dynamics in the O-CN land surface model: 1. Model description, site-scale evaluation,  
 700 and sensitivity to parameter estimates, *Global Biogeochemical Cycles*, 24, <https://doi.org/https://doi.org/10.1029/2009GB003521>, <https://agupubs.onlinelibrary.wiley.com/doi/abs/10.1029/2009GB003521>, 2010.